Recent Advances in Research of Lightning Meteorology

QIE Xiushu[1,2]* (郄秀书), LIU Dongxia[1,2] (刘冬霞), and SUN Zhuling[1] (孙竹玲)

1 *Key Laboratory of Middle Atmosphere and Global Environment Observation (LAGEO), Institute of Atmospheric Physics, Chinese Academy of Sciences, Beijing* 100029

2 *Collaborative Innovation Center on Forecast and Evaluation of Meteorological Disasters, Nanjing University of Information Science & Technology, Nanjing* 210044

(Received March 26, 2014; in final form July 3, 2014)

ABSTRACT

Lightning meteorology focuses on investigating the lightning activities in different types of convective weather systems and the relationship of lightning to the dynamic and microphysical processes in thunderstorms. With the development and application of advanced lightning detection and location technologies, lightning meteorology has been developed into an important interdiscipline between atmospheric electricity and meteorology. This paper mainly reviews the advances of lightning meteorology research in recent years in China from the following five aspects: 1) development of advanced lightning location technology, 2) characteristics of lightning activity in different convective systems, 3) relationship of lightning to the dynamic and microphysical processes in thunderstorms, 4) charge structure of thunderstorms, and 5) lightning data assimilation techniques and application to severe weather forecasting. In addition, some important aspects on future research of the lightning meteorology are proposed.

Key words: lightning activity, lightning detection, charge structure, lightning assimilation, convective weather system

Citation: Qie Xiushu, Liu Dongxia, and Sun Zhuling, 2014: Recent advances in research of lightning meteorology. *J. Meteor. Res.*, **28**(5), 983–1002, doi: 10.1007/s13351-014-3295-0.

1. Introduction

Lightning accompanies strong convective weather systems. As such, not only it is closely related to development of the dynamic and microphysical processes in such systems, but is also an indicator of their initiation and development. Through the interaction of appropriate dynamic and thermodynamic conditions and terrains, cumulonimbus clouds form in unstable convective environments, accompanied by strong up- and down-drafts, creating a thunderstorm. The charge separation and transfer between different hydrometeor particles with varying speeds result in formation of oppositely charged regions, leading to the occurrence of lightning. Lightning meteorology has mainly focused on investigating the lightning activities in different types of strong convective weather systems, and the relationship of lightning to the dynamic and microphysical processes in a thunderstorm. The primary application of lightning meteorology is convective weather warning and forecasting.

Observational data derived from experiments based on advanced lightning location technology are the basis of understanding of lightning activity characteristics in severe convective weather systems, and are used in forecasting of severe convective weather. This paper first reviews development of the advanced lightning location technology; then introduces the characteristics of lightning in different convective systems, the relationship of lightning to the dynamic and microphysical processes in a thunderstorm, and the charge structure of thunderstorms; and finally reviews lightning data assimilation and its application to severe weather forecasting.

Supported by the National Key Basic Research and Development (973) Program of China (2014CB441401) and National Natural Science Foundation of China (40930949).

*Corresponding author: qiex@mail.iap.ac.cn.

©The Chinese Meteorological Society and Springer-Verlag Berlin Heidelberg 2014

2. Development of lightning location technology

With development of the electronic and information technology, many countries such as the United States (US), France, and China have successively developed advanced lightning location systems since the 1970s. For example, the well-developed cloud-to-ground (CG) lightning detection networks since the late 1970s, the very high frequency (VHF) lightning radiation source location system that accurately maps the lighting discharge processes since the 1990s, the World-Wide Lightning Location Network (WWLLN), and the space-based lightning detection sensors aboard the satellites. These lightning detection technologies have been improved continuously, and are applied in many significant international research programs. For example, the Severe Thunderstorm Electrification and Precipitation Study (STEPS) conducted in the American Great Plains in 2000, the Thunderstorm Electrification and Lightning Experiment (TELEX) in 2004, and a 10-yr (2010–2020) weather observation plan, Hydrological cycle in the Mediterranean Experiment (HyMEX) project launched by France, etc. All of these projects used the lightning VHF radiation source location technology in three dimensions (3D) with high temporal and spatial resolutions. Based on the comprehensive observations using advanced lightning location technology, the integrated observation data with high temporal and spatial resolutions can be obtained. Then, the lightning activity in different convection systems and the relationship of lightning to the dynamic and microphysical processes in a thunderstorm can be investigated, which is an active research field in the current atmospheric electricity. This line of research also promotes the application of lightning data in the monitoring and forecasting of catastrophic weather.

2.1 Ground-based lightning location

Lightning discharges emit electromagnetic radiation in broadband frequency ranges, which is strong in the radio spectrum and even detectable in the high-energy radiation spectrum (X-ray and Gamma-ray). The electromagnetic radiation provides an important signal to detect and locate lightning discharges. As the most widely used lightning location system, the crossed-loop magnetic direction finders (DF) working in the very low frequency/low frequency (VLF/LF) range was first developed by the University of Arizona in the 1970s. The system could recognize the CG lightning flashes by using the feature of electromagnetic field waveforms produced by the return stroke, and then locate the CG flashes effectively. With the development of the Global Positioning System (GPS), the IMPACT (improved accuracy from combined technology) algorithm was proposed as a combination of DF and the time-of-arrival (TOA) technology. Based on the IMPACT, the commercial US National Lightning Detection Network (NLDN) was first operated (Cummins et al., 1998), and then similar lightning detection networks were set up in many areas and countries, such as North America, South America, Europe, and China. The detection efficiency of the NLDN reaches about 95%, the corresponding location precision is better than 500 m, and the time precision is about 1 ms (Biagi et al., 2007). Similar lightning detection networks were established by the China Meteorological Administration and the Chinese Electric Power Companies. The CG location system provides information of time and location of the return strokes, and the peak current is estimated by using the peak value of the measured magnetic field. In the 1980s and 1990s, the CG lightning location systems played an important role in the study of lightning activities in severe convective weather systems (e.g., Reap and MacGorman, 1989; Qie et al., 1993).

Based on the long-baseline TOA lightning location technology, the Lightning Mapping Array (LMA) was designed by the New Mexico Institute of Mining and Technology (Rison et al., 1999), and has become the most precise location system in 3D across the world. The center frequency was originally 63 MHz with a bandwidth of 6 MHz, and now the center frequency is adjustable in the VHF band to avoid the background radio frequency interference. Total lightning, including both the CG lightning (less than 1/3 of the total) and the intra-cloud (IC) lightning (more than 2/3 of the total), can be imaged in 3D, and the progression of lightning discharges can also be depicted in detail. The nonlinear least-square regression algorithm is applied in the 3D location of the radiation sources. The LMA determines hundreds to thousands of radiation events per lightning flash, and accurately maps the progression structure of lightning discharge in 3D. The LMA has been widely utilized as the major detection technology in many research programs related to severe convection storms in the US and Europe, such as STEPS, TELEX, DC3 (the Deep Convective Clouds and Chemistry Project), and HyMEX. The US Lightning Detection and Ranging (LDAR II) system adopts the similar location principle as the LMA with two adjustable frequency bands (60–66 and 222–228 MHz), and is another lightning VHF radiation location system with high detection efficiency and location precision in 3D.

In China, the Lightning Mapping System (LMS) has also been designed based on the long-baseline TOA technique, similar to the LMA in the US. The center frequency of the system is 270 MHz. The horizontal error is less than 11 m and the altitude error is 2–3 times greater, when lightning occurs inside or about 10 km near the network with an altitude between 4 and 15 km. The altitude error increases with the reduction of the radiation source height (Zhang et al., 2010). Figure 1 shows the 3D location result of an IC lightning detected by the LMS. It is found that the lightning was initiated from the lower negative charge region, and propagated upward into the upper positive charge region. Subsequently, the lightning channels spread horizontally in both charge regions. At present, the LMS is only used in scientific research, while has not yet supported the real-time and continuous location over the duration of an entire thunderstorm. Therefore, it cannot be applied to operational monitoring of the lightning activity in severe convective storms.

SAFIR (System d'Alerte Fondre par Interferometrie Radio electrique) initiated in France is a lightning VHF detection and location system based on the interferometry technique. The center frequency of the system is adjustable within the range of 110–118 MHz and a bandwidth of 1 MHz. The SAFIR determines the lightning radiation sources in 3D, and reproduces the progression of lightning discharge channels. Meanwhile, the LF electric field antenna is integrated to distinguish the IC and CG lightning according to the electric field signals from 300 Hz to 3 MHz (Richard et al., 1986). Using data from the Beijing SAFIR3000 lightning detection system and Doppler radar, Liu et al. (2011) analyzed the temporal evolution of lightning radiation sources in a leading-line and trailing stratiform mesoscale convective system (LLTS-MCS) over Beijing, and found that the radiation sources over the central detection network had a good agreement with the radar echo, while the altitude error of many radiation sources appeared relatively large.

In addition, there are other lightning VHF location systems, including the narrowband interferometer (Zhang et al., 2008) and broadband interferometer (Dong et al., 2002) based on the interferometry technique, and the lightning VHF radiation location system based on short-baseline time-difference of arrival technique (Cao et al., 2012; Sun et al., 2013). Most of the systems have merely realized the 2D location or finite 3D location (Wu et al., 2012), and the coverage areas are relatively small. Therefore, these systems are only applied in the study of lightning physics.

The WWLLN is operated in the VLF range (3–30 kHz), with the center station established in the University of Washington. The network could effectively detect the electromagnetic radiation emitted by the lightning discharge at thousands of kilometers away. With about 60 ground-based observations around the world, the WWLLN detects global lightning activities continuously. With a GPS antenna for accurate arrival time of the lightning impulses, the WWLLN locates the lightning based on the time-of-arrival technique (Dowden et al., 2008). Due to the lower operating frequency and fewer numbers of stations, the detection precision and efficiency of WWLLN were very low, and the detection precision was about 10 km. With increasing WWLLN station numbers, the detection efficiency of the WWLLN has increased from 3.88% in 2006–2007 to 10.30% in 2008–2009. Besides, there are also other VLF/LF lightning location networks, for example, the Los Alamos Sferic Arrays (LASA) in America (Smith et al., 2002), Lightning Detection Network in Europe (LINET; Betz et al., 2009), and Beijing Lightning Network in China (BLNet; Wang et al., 2009).

2.2 *Space-based optical lightning location*

The Lightning Imaging Sensor (LIS) aboard the Tropical Rainfall Measuring Mission (TRMM) is des-

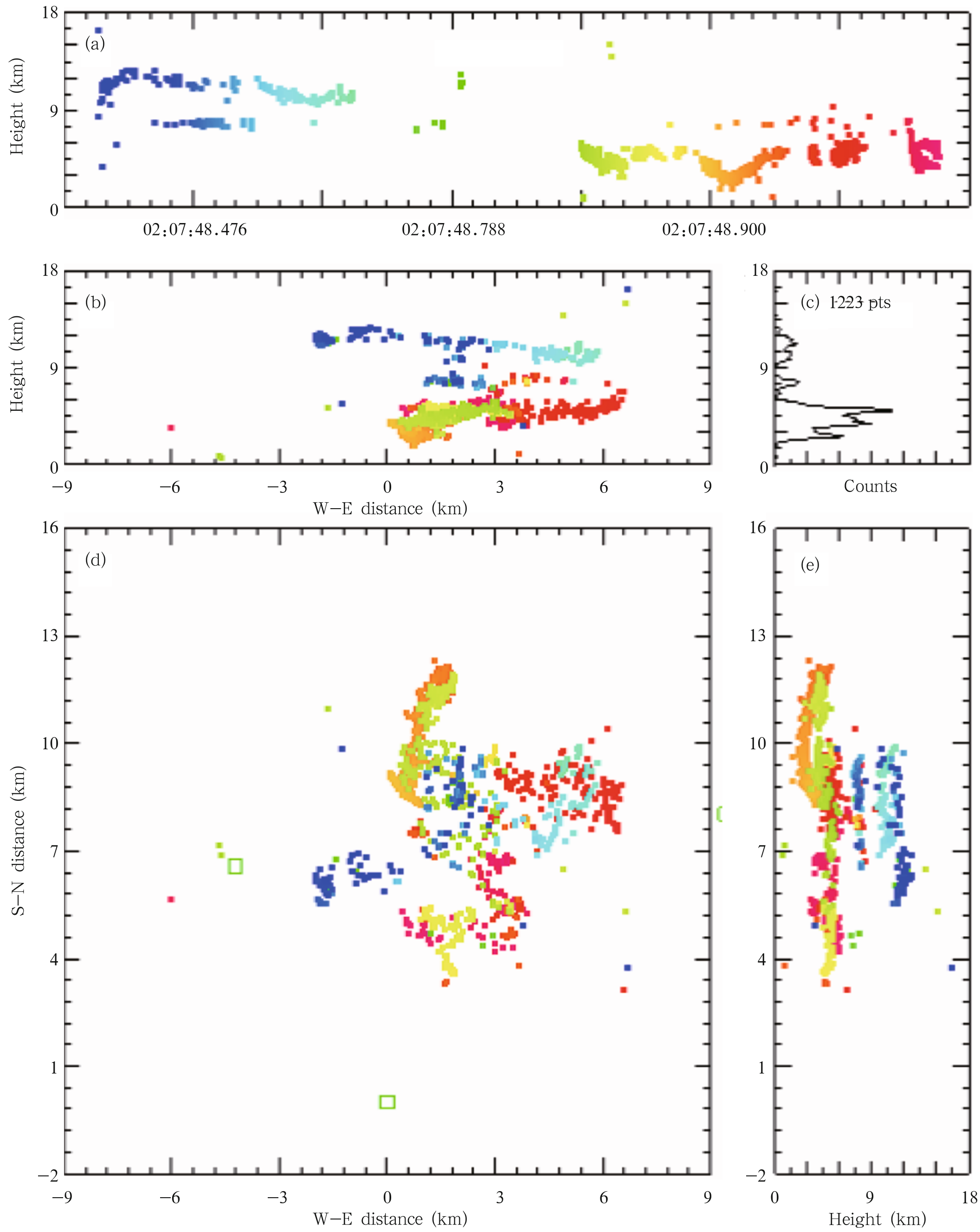

Fig. 1. The 3D location of an IC lightning detected by LMS. (a) The height of lightning radiation versus time, (b) east-west (W-E) vertical projection, (c) the number of lightning radiation sources versus height, (d) plan view, and (e) south-north (S-N) vertical projection. Different colors stand for time evolution. The discharge started in blue. [Adapted from Zhang et al., 2010]

igned to monitor the characteristics of total lightning activity in severe convective weather. The LIS observes the lightning activity between 35°S and 35°N with a view of 600 × 600 km^2 area on the earth, and the spatial resolution is about 3–6 km. The view time for an individual storm or storm system is about 90 s. As a similar optical sensor before LIS, the Optical Transient Detector (OTD) on the Mictolab-1 satellite observes an area of 1300 × 1300 km^2 in 70° inclination orbit. The spatial resolution is 10 km, and the temporal resolution is 2 ms. The detection efficiency of the OTD is between 50% and 66%. For LIS, the IC and CG lightning cannot be distinguished, while continuous observation is available day and night. Boccippio et al. (2002) compared LIS and LMA observation data, and found that the lighting location results from the two datasets were well consistent in space and time. The IC lightning occurs at middle–upper levels of the storm, which is easier to be detected by the LIS than the CG lightning, and the LIS tends to detect the latter period of the CG lightning. The LIS detection efficiencies near local noon and near local overnight are about (73±11)% and (93±4)%, and location errors for IC and CG lightning are about 4 and 12 km, respectively.

Although there are significant differences between OTD and LIS in the spatial resolution and observation regions, NASA researchers have combined and averaged the two sensors' data to create a global lightning activity database spanning from May 1995 up to now, which is the first lightning database with long time and high precision in the world. For the database, not only the temporal-spatial changes in instrument detection efficiency are considered, the different view time of the sensors in different latitudes is also corrected. Figure 2 shows the lightning distribution of the world from May 1995 to February 2012 by LIS/OTD. It is obvious that lightning activity over land is far more than that over ocean, and the lightning density ratio of land to ocean is about 10:1 (Zhu et al., 2013). The LIS, the precipitation radar (PR), TRMM Microwave Imager (TMI) and other sensors on the TRMM can be combined together to provide information on the characteristics of lightning activity, precipitation, and microphysical processes in different severe convective weather systems.

3. Lightning activity in different convective systems

The development of lightning detection technology has greatly improved the understanding of light-

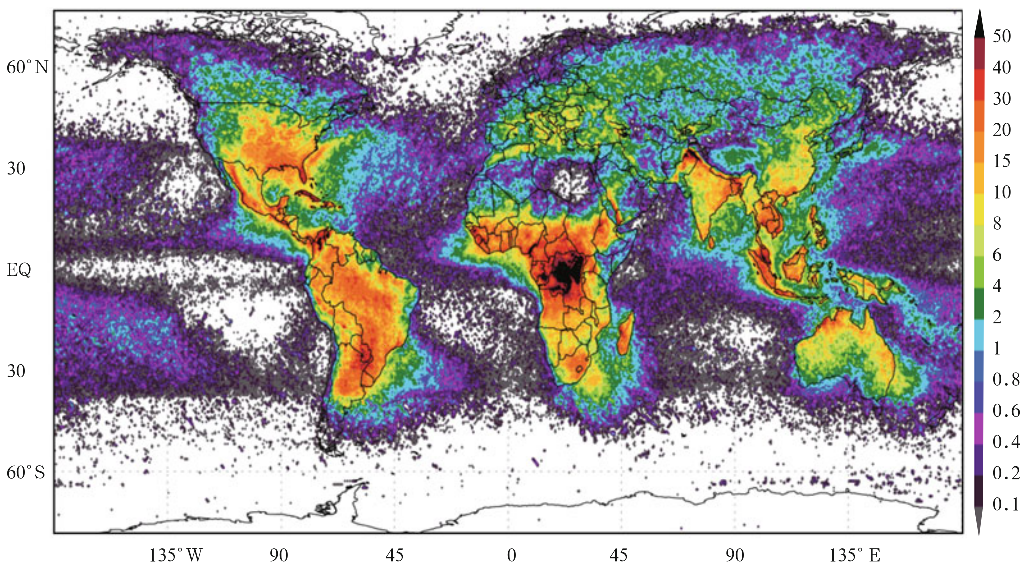

Fig. 2. Lightning (fl yr^{-1} km^{-2}) distribution across the globe from May 1995 to February 2012 by LIS/OTD. [From Qie et al., 2013]

ning activity in thunderstorms. Combined data from the lightning detection network, Doppler weather radar, and satellites have been particularly useful. The gradual development of the CG lightning detection network in the US since the late 1970s has enabled the characterization of CG lightning activities of convective weather systems, based on the lightning location data including both IC and CG lightning observed by lightning detection systems such as SAFIR, LDAR and LMA, WWLLN, and satellite (LIS/OTD). The lightning activities in convective weather with different precipitation characteristics have been investigated, such as squall line, supercell, hailstorm, typhoon, etc. (Qie et al., 2005, 2006; Zhang et al., 2006a; Qie, 2012). We next separately consider in detail the different types of precipitation systems that may accompany lightning.

3.1 Lightning characteristics of hailstorm

Generally, the frequency of –CG (negative CG) lightning is higher than +CG lightning during the lifecycle of a thunderstorm, but hailstorms are usually accompanied by a higher ratio of +CG lightning (Carey and Rutledge, 1998; Feng et al., 2006; 2007; Liu et al., 2009). Based on CG lightning location, radar, and TRMM/LIS data, Feng et al. (2007) observed that the +CG lightning accounted for a high percentage of total lightning over the lifetime of a hailstorm, with the hail-falling stage coinciding with the most rapid increase of +CG lightning. Using total lightning detected by SAFIR3000 and radar data, Zheng et al. (2010) found that +CG lightning frequency and hail fall were correlated. Therefore, the +CG lightning frequency may indicate the occurrence of hail fall. However, Soula et al. (2004) analyzed the lightning activity of hailstorms in the south of France, and demonstrated that the CG lightning frequency was no more than 2 fl min^{-1} (flashes per minute): far less than that expected in a rain-generated storm, where the lightning frequency was 12 fl min^{-1}. This result showed that +CG lightning frequency alone may not reliably identity hailstorms.

Severe weather events, including hailstorms, are often accompanied by frequent lightning activities. A rapid increase in total lightning frequency indicates the occurrence of severe weather events. Schultz et al. (2011) analyzed 711 thunderstorms that occurred in four different regions of the US. Their large sample size resulted in good representation for all severe thunderstorm types. They included tornado-produced storms, those where the hail diameter exceeded 1.9 cm, and those where the wind speed exceeded 26 m s^{-1}, and also weak thunderstorms. They tested the ability of monitoring the rapid increase of total lightning and CG lightning to forecast severe weather events, using the method of 2σ lightning jumping (the rate of change of the total flashes rate; DFRDT). Both the total and CG lightning were found to increase before the occurrence of severe weather events, but the forecasting ability of total lightning flashes was more effective than CG lightning, with the total lightning of 20.65 min and CG lightning of 13.54 min. Yao et al. (2013) studied the hailstorms in the Beijing area, and found that the 2σ lightning jumping method (+CG lightning and total lightning) could also be successfully applied to hail forecasting in that region.

3.2 Lightning activity in linear mesoscale convective systems

Linear mesoscale convective systems (MCSs) are severe convective weather systems occurring frequently in summer, and are also known as squall lines. Using radar morphology, Parker et al. (2000) divided linear MCSs into three categories: leading stratiform (LS-MCS), trailing stratiform (TS-MCS), and parallel stratiform (PS-MCS). They found that LS-MCSs produced more +CG lightning than the other two types. Further observational studies found that the –CG lightning dominated at the mature stage of a linear MCS, and +CG lightning occurred relatively frequently in the stratiform region at the dissipating stage (Parker et al., 2000; Feng et al., 2009). Case studies of the lightning VHF source location showed that the total lightning frequency of a linear MCS increased from 130 to 600 fl min^{-1} (Lang and Rutledge, 2008; Liu et al., 2013a, b). Yuan and Qie (2010a) studied a squall line that occurred in South China using TRMM/LIS data, and found that the instant lightning frequency reached a maximum of 567 fl min^{-1} during the satellite pass over. This result suggested that the lightning activities of squall line systems are more active than normal thunderstorms (Yuan and Qie, 2010b) because of a wide range of strong convection. Using an SAFIR3000 lightning location system, Liu et al. (2013a) analyzed a linear MCS over Beijing. Their results showed that lightning activity was correlated with radar data and precipitation. Figure 3, reproduced from that work, indicates that lightning was concentrated over the strong convection area, while fewer lightning flashes occurred in the stratiform region, and most of them were +CG lightning.

Carey et al. (2005) used LDARII data to examine lightning activity in a linear MCS and obtained the fine structure of IC lightning extension. They found that the lightning radiation sources had a two-layer distribution, sloping from the convective layer to the stratiform region as shown in Fig. 4. To a certain extent, the results reflected the charge distribution in the lightning discharge of linear MCSs.

A positive charge in the stratiform region of a linear MCS may form via either the charge advection from the convective region or the local electrification mechanism. The charge advection mechanism happens when ice crystals in the stratiform region become positively charged through the advection of upper airflow from the convective region. Figure 4 shows the lightning radiation source distribution, which correlates well with the trajectory of ice particles sinking in the MCS shown in Fig. 5. Since ice particles are the primary positive charge carriers, the charge moves from the convective region to the stratiform region by the advection of upper airflow of the thunderstorm. The local electrification mechanism occurs when in-

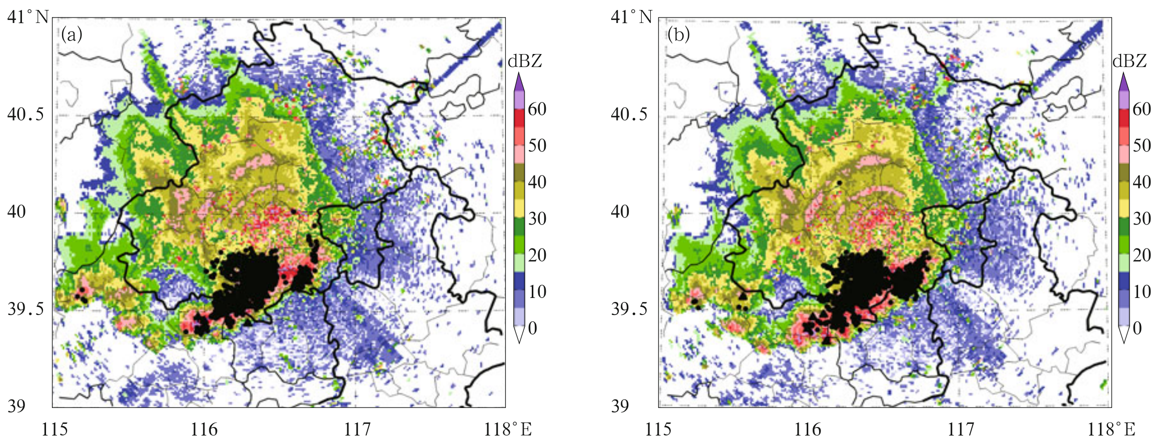

Fig. 3. Composite radar reflectivity and the lightning location within six minutes at two times of a leading line MCS. Black dots represent lightning flashes. [From Liu et al., 2013a]

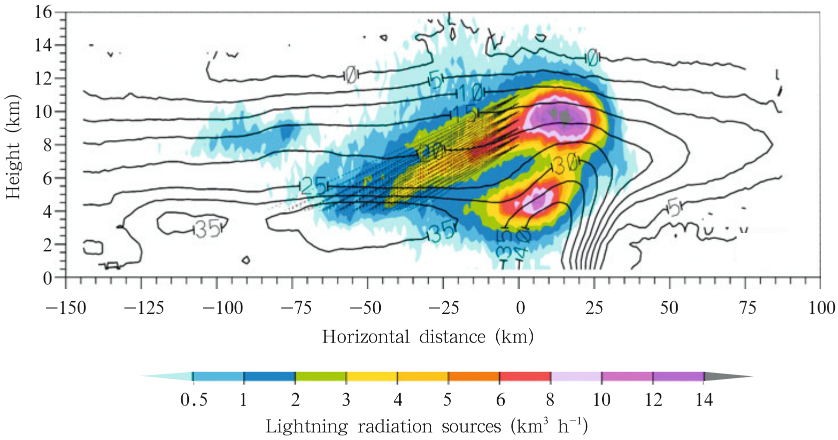

Fig. 4. Lightning radiation sources detected by VHF (shading) and radar reflectivity (contours) of a typical linear MCS. [Reproduced from Carey et al., 2005]

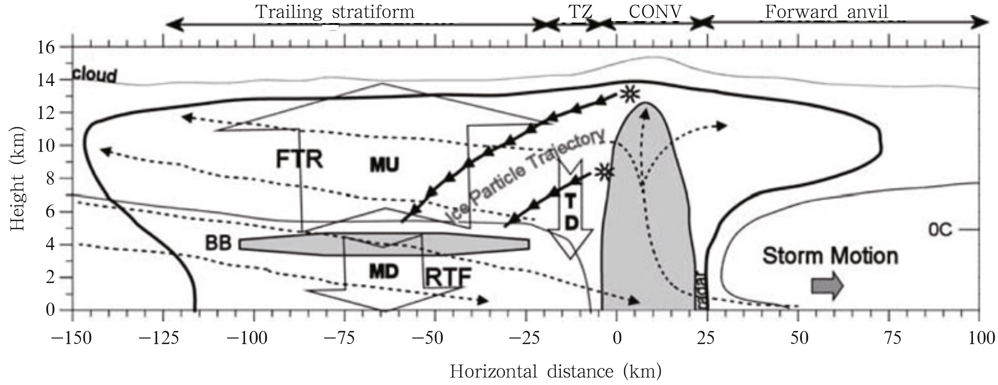

Fig. 5. An MCS conceptual model. [From Carey et al., 2005]

situ charge separation happens within the stratiform region, through ice particle collisions. Dotzek et al. (2005) found that both the horizontal propagation of discharge sources and a radar reflectivity factor above the 0℃ bright band in the mixed phase area were increased, confirming a local electrification mechanism in the stratiform region.

Transient luminous events (TLE) usually occur over the MCSs (Pasko et al., 2002; Yang et al., 2008, 2013a, b). Red sprites are thought to be induced by +CG lightning in the stratiform region of an MCS. Lu et al. (2009) discussed the charge moment changes of the sprite-producing +CG lightning, typically 1500–3200 C km^{-1}, which is much greater than that of normal CG lighting. Yang et al. (2013a, b) compared the sprite-generated MCS to other thunderstorm types, and suggested that the convection was stronger in sprite-generated thunderstorms, but there was no obvious difference in the microphysical characteristics.

3.3 Lightning activity in typhoons

Although lightning in tropical cyclones varies, the mean lightning density presents an obvious three-circle structure during most of the typhoon stage (Molinari et al., 1994; Pan et al., 2010; Zhang et al., 2012). The peak lightning density appears in the outer rain band. A lower lightning frequency is found in the eyewall region, and lightning frequency trends to be zero in the inner rain band. Figure 6 shows that the lightning occurring in the outer rain band has an asymmetric distribution, with the highest density mainly located in the deep convection area.

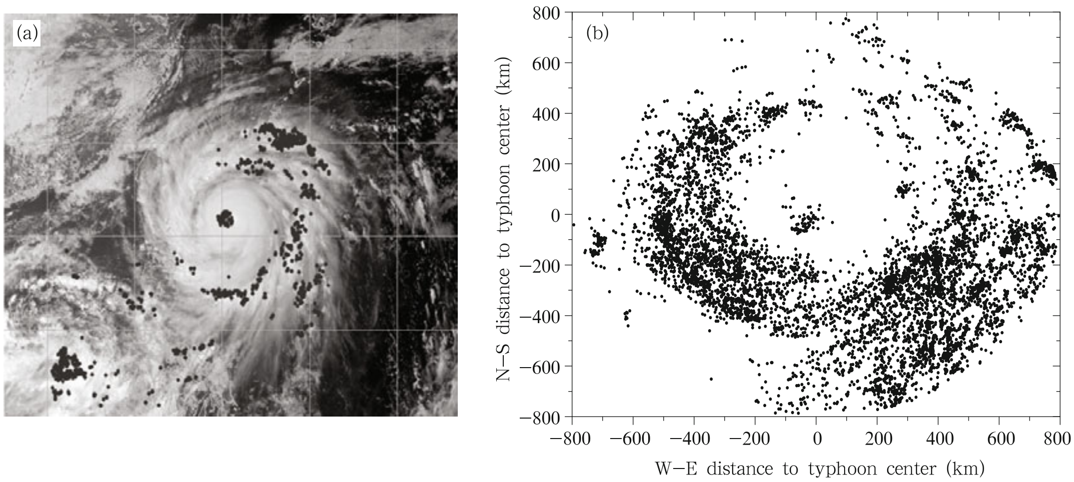

Fig. 6. Lightning distribution in Typhoon Qiangwei. (a) Lightning (dark dots) during 0200–0600 UTC 27 September 2008, superimposed over visible cloud imagery from GMS-6 data at 0600 UTC, and (b) composite lightning distribution at the mature stage of Typhoon Qiangwei.

The lightning density at the cyclone center is higher while the storm strengthens than at the weakening stage (Abarca et al., 2011). Generally, the lightning in the eye wall of a typhoon increases sharply as the wind speed reaches its maximum, so the lightning density in the eye wall could indicate the intensity of a strengthening typhoon (Pan et al., 2010). Price et al. (2009) analyzed lightning data detected by WWLLN for 58 hurricanes during 2005–2007, and showed that lightning frequency and hurricane strength (i.e., maximum sustained winds) were positively correlated, with an average correlation coefficient of 0.86. Pan et al. (2014) studied lightning in 69 tropical cyclones over Northwest Pacific, and found that in more than half of the weak (levels 1–3) and strong (levels 4–5) typhoons, the peak value of lightning usually occurred before the maximum wind speed was attained. Yang et al. (2011) analyzed lightning during different intensity stages of 46 tropical cyclones using the distribution characteristics of radar reflectivity and ice scattering from the TRMM data, and found that the spatial distribution of lightning differed for storms at different intensities. Diurnal variation of lightning above the sea has been shown to have two peak values, occurring respectively in the afternoon and morning (Pan et al., 2013).

3.4 Compact intra-cloud discharge and strong convection

In the last two decades, a special type of lightning discharge named CID (Compact Intra-cloud Discharge) or NBE (Narrow Bipolar Event), has caused widespread concern. CIDs are different from regular lightning discharge processes. This kind of discharge has a small discharge scale and a short duration of about 10–20 μs, with extremely strong high and low frequency radiation, one order of magnitude larger than that of regular intra-cloud discharge (Smith et al., 1999; Zhu et al., 2007, 2010; Wang et al., 2012). Based on 3D CID location results, Wu et al. (2011) found that the discharge height of negative CIDs was generally comparable to that of the tropopause, and the negative CIDs were much less abundant than positive CIDs. These results indicated that negative CIDs were probably produced in extremely vigorous thunderstorm processes, and may therefore reveal strong convective activity. CIDs tend to occur at top and middle levels of thunderstorms. These discharges can be produced not only in regions with strong radar echo, but also in regions with lower than 30-dBZ radar echo in the later stage of a thunderstorm. The height of CIDs might be related to the ionosphere height, but no significant relation has been found. Using LMS, Wang et al. (2012) analyzed 236 CIDs observed in Binzhou, Shandong Province during the summers of 2007–2008, and found that CIDs occurred at altitudes between 7 and 16 km with a peak power ranging between 12 and 781 kW in the 267–273-MHz band. Lü et al. (2013) reported that NBEs in the Daxing'anling region tended to occur during the relatively active period of lightning discharges. NBEs tended to cluster around the area of a particular convective core with high radar echo, and most gathered at the front area of convective cores. The position of NBEs moved consistently with the movement of the particular convective cores.

4. Relationship of lightning to dynamic and microphysical processes and precipitation

Strong convective weather systems are characterized by dynamic, microphysical, and electrochemical processes. Dynamic processes are characterized by strong updrafts, down bursts, and horizontal wind shear. Microphysical processes include all kinds of particle growth and phase change. The electrical processes denote electrification, charge distribution changes, and discharge process. All of these processes influence each other. Usually, lightning occurs where an updraft is strong enough to support the coexistence of a mixed phase region with graupel and liquid water. Carey and Rutledge (1998) found that CG lightning had a very close relationship with graupel. CG lightning was generally located in a strong radar echo region, but was not completely consistent with the strong updraft. Based on radar data, lightning detection and electric field sounding, Bruning et al. (2007) observed a multi-cell thunderstorm. They proved that there were many graupel particles at the occurrence of the first lightning, and that the strong electric field was caused by electrification from ice particle collisions in the updraft. Lightning frequency and ice particle content were positively correlated.

Zhou et al. (2002) found that lightning and convective precipitation were correlated, and lightning could therefore be used to estimate precipitation in general convective weather. Meanwhile, lightning frequency and unstable stratification maximum energy could indicate the occurrence and development of convectional weather (Zhou et al., 1999). Feng et al. (2007) combined ground-based radar and lightning location data with LIS, PR, and TMI data from the TRMM satellite, and found that convective precipitation comprised more than 85% of the total precipitation in hailstorms, and the correlation of the lightning and convective precipitation could be used to identify the convective precipitation area effectively. Based on multi-sensor data from the TRMM satellite, Yuan and Qie (2010a) studied lightning activity and its relationship with the precipitation structure of a strong squall line in South China, and found that the majority of lightning occurred in the convective region. The vertical profile of the maximum radar reflectivity of the convective cell may be a good indicator of lightning frequency and convective intensity. For the cell accompanied by the highest frequency of lightning, the radar reflectivity at each height level was usually the largest, and the reflectivity lapse rate was the smallest over the frozen layer, and vice versa, for the cell with the lowest frequency of lightning. Zheng et al. (2004) analyzed a frontal cyclone system that occurred in the Huaihe River basin, and the results showed that lightning occurred in the strong convective precipitation cloud influenced by the cold front; no lightning occurred in the warm front. Precipitation profiles with high lightning frequency usually contain a high density of ice particles. The precipitation profile of a thunderstorm with different lightning frequency is different. The higher lightning frequency corresponded to the greater precipitation above 5-km height inside the thunderstorm. Hence, thunderstorms with more frequent lightning had more ice particles above the frozen layer (Ma et al., 2012).

To realize lightning parameterization in a global or mesoscale model, it is necessary to obtain a quantitative relation between the lightning activity and the dynamic and microphysical parameters of the thunderstorm. Research in this area has most recently used the TRMM satellite multi-sensor data. Yuan and Qie (2008) found that lightning frequency and parameters of thunderstorms, such as the top of thunderstorm, frozen layer thickness, and minimum temperature, showed an exponential relationship; for both a precipitation system or a convective cell, the relationship between lightning frequency and ice-phase precipitation content from 7 to 11 km remained relatively stable, and the correlation coefficient was greater than 0.7. Their work provides a possible lightning parameterization scheme that might be used widely in regional or global models.

5. Charge structure of a thunderstorm: Observation and simulation

An essential technique in lightning and thunderstorm research is electric field sounding. This method has the major advantage of directly detecting the electric field inside a thunderstorm, and reflecting the vertical distribution of the charge along the sounding path. Electric sounding experiments have played an essential role in recognizing the charge distribution of different thunderstorms, and promoting the research of thunderstorm electrification mechanism, charge structure and its relationship with storm dynamics and lightning initiating mechanisms (Marshall et al., 1995; Stolzenburg et al., 1998).

5.1 Sounding of the charge structure inside a thunderstorm

In as early as 1937, Simpson and Scrase (1937) obtained direct scientific evidence of the tripole charge structure inside thunderstorms by using the electric field sounding. This simplified tripole charge structure model remained widely accepted for more than half a century. More recent electric field sounding data have shown that the real charge structure is much more complex for most of the thunderstorms. Marshall et al. (1995) observed 11 electric field soundings and corresponding thermodynamic parameters for multicell and supercell thunderstorms in the southern Great Plains of the US. They found that the charge structure in the weak updraft area was complex, with 7–9 charge regions below 10 km, while the charge structure was simple in the strong updraft area with 3–5 charge regions below 10 km. Using 49 electric field soundings, Stolzenburg et al. (1998) investigated three categories of thunderstorm system, including MCSs, supercells in the southern Great Plains, and small thunderstorms in New Mexico mountain region of the US. Their results showed that the convective regions of the three types of thunderstorms had the same basic charge structure: in the updraft area there were four vertical, alternating polarity charge regions and the lowest charge zones were positively charged. Figure 7 graphically displays their findings. The charge structure outside the updraft region (still in the convective region) included six vertical alternating polarity charge regions, with the lowest charge region still positively charged. The height of the basic charge regions inside the three thunderstorms increased in line with the updraft of the thunderstorm.

Tessendorf et al. (2007) revealed the existence of inverted charge structure of thunderstorms. Using 3D LMA data from the STEPS experiment, they analyzed lightning radiation sources of two thunderstorms, and found that one thunderstorm showed a normal tripole charge structure with the middle layer negatively charged. Although the upper negative shield charge region was not reflected, the charge structure was consistent with electric field sounding results in view of the charge region involved in the discharge. The other thunderstorm had an inverted charge structure with positive charge at the middle level, opposite to a normal charge structure. The inverted charge structure usually occurred in supercell storms, accompanied by tornadoes or other disastrous weather (MacGorman et al., 2005). Zhang et al. (2004) utilized the LMA lightning data to analyze the lightning characteristics of a supercell storm and found that the spatiotemporal distribution of lightning holes and rings corresponded to updrafts and downdrafts. Lightning holes usually appeared before a tornado, and became most obvious during the tornado stage. During the period of high frequency +CG lightning, the main convective region of the thunderstorm had an inverted tripole charge structure, with +CG lightning produced by the positive charge at the middle level. The –CG lightning was mainly located in the anvil region of the thunderstorm. The cloud anvil showed a dipole charge structure, and a high frequency of –CG lightning was generated in the upper negative region (Zhang et al., 2004).

Over the inland plateau of China, thunderstorms often present with a special charge structure. Qie et

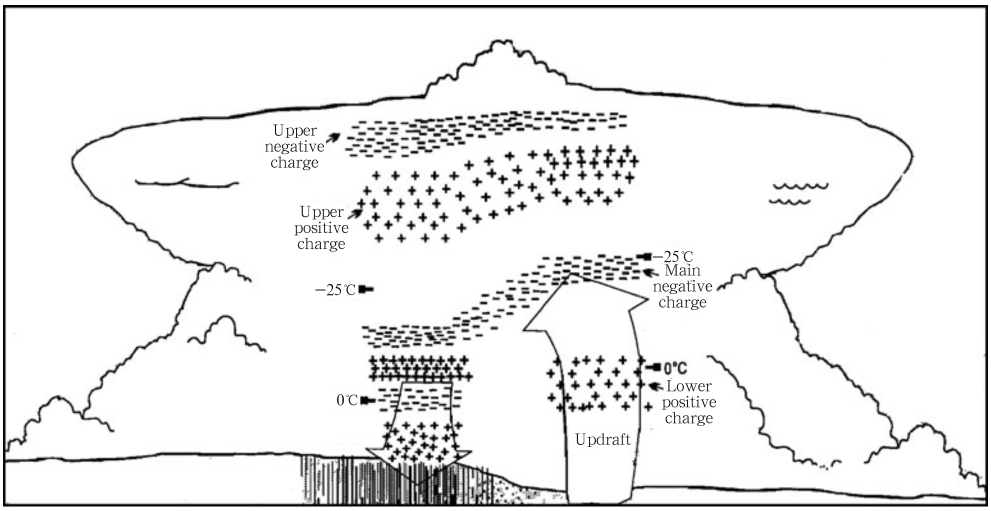

Fig. 7. Conceptual model of the charge structure in the convective region of a thunderstorm. [From Stolzenburg et al., 1998]

al. (2005, 2009) comprehensively analyzed the surface electric field and lightning charge source location of a large number of thunderstorms. Some thunderstorms showed an abnormally large positive charge at the lower level, and the proportion of this type of thunderstorms gradually increased with average altitude, adding to the evidence for the predominance of larger lower positive charge region (Liu et al., 1989). Based on corona probe sounding techniques, the charge structure of a thunderstorm that occurred in Gansu Province, China was observed by Zhao et al. (2009). Their results showed that the thunderstorm presented a negative charge region at the middle level, and positive charge regions at the upper and lower levels with the lower positive region larger than the normal tripole, further confirming the abovementioned conclusions. Recently, based on 3D localization of wideband electric field change pulses, Li et al. (2013) analyzed the charge structure of a thunderstorm in Qinghai Province, China. They found an inverted dipole charge structure at the development and mature stage of the thunderstorm, with four charge layers (positive-negative-positive-negative) at the dissipating stage, at heights of 5.0, 4.0, 3.0, and 1.8 km, respectively.

5.2 Simulation of charge structure in thunderstorms

Increasing computing speeds have made it possible to study thunderstorm electrification and discharge processes by using high resolution numerical simulations. The simulation of dynamic-electrification coupling has already become an important research topic. There are three main advantages of simulations. First, complex interaction of the microphysical processes with the electrification, discharge, and dynamic processes can be unraveled. Second, simulations can provide high spatiotemporal resolution data for different physical processes, going some way to remedy the deficiency of thunderstorm observations. Third, all kinds of electrification, discharge mechanisms, and theoretical hypotheses can be effectively and economically verified.

The noninductive electrification mechanism is considered to be the major electrification mechanism in strong convective weather (Takahashi, 1978; Saunders et al., 1991). In this mechanism, charge separation is caused by bouncing collisions between large and small ice particles in the mixed phase region, and does not require an external electric field. The noninductive electrification mechanism results in a fast charging rate. Moreover, the reversal temperature, which affects the polarity of charge transferred, is a key factor in determining the charge structure. The inductive electrification mechanism of hydrometeor particles dependent on the environmental electric field also plays an important role at the initial stage of the electrification of thunderstorms.

With the gradual improvement of models and increased availability of observational data, the simulated charge structure of thunderstorms has become increasingly accurate. Mansell et al. (2005) compared five different noninductive electrification schemes, using a 3D thunderstorm model that considered both the inductive and the noninductive electrification mechanisms. They found that three had a normal tripole charge structure (negative region in the middle), while the other two were mainly dependent on the riming of graupel particles. Although lightning propagation and breakdown processes are relatively complicated, it is possible to establish lightning discharge parameterization schemes on the basis of the electrification model with a high temporal and spatial resolution. A large number of studies on charge structure and discharge processes were based on the thunderstorm model developed from hailstorm models in China (Yan et al., 1996; Zhang et al., 2000; Sun et al., 2002; Tan et al., 2007). The simulation of real thunderstorms is also gathering attention of more researchers (Guo et al., 2007; Zhou and Guo, 2009; Liu et al., 2014). Tan et al. (2006) adopted the lightning parameterization from Mansell et al. (2002) into a 2D high resolution thunderstorm model, and the lightning discharge channel structure and propagation characteristics were reproduced well. The model resolution reached 12.5 m, and the simulation results well represented the discharge characteristics of the channel and the development of bi-directional leaders.

In order to simulate large-scale thunderstorms more realistically, simulations of charge structure based on the mesoscale NWP (numerical weather prediction) models have been developed in recent years. Huang et al. (2008) simulated lightning activity by coupling electrification and discharge processes in the mesoscale model GRAPES (Global/Regional Assimilation and Prediction System) of China, which provided a background field for a nested cloud-scale model. Li et al. (2012) and Liu et al. (2014) introduced two noninductive electrification schemes. Takahashi (1978; abbreviated as Takahashi78) and Saunders and Peck (1998; abbreviated as Saunders98) implanted lightning discharge parameterization schemes into the RAMS (Regional Atmospheric Model System) model v6.0, and found that the simulated thunderstorm showed a tripole charge structure under the Takahashi78 electrification scheme and changed from a dipolar to tripolar charge structure under the Saunders98 scheme. The simulated lightning frequency was consistent with observation. Xu et al. (2012) simulated the charge structure of a supercell in the WRF (Weather Research and Forecasting) model, which was coupled with electrification and discharge processes. The results showed a tripolar charge structure with a positive charge region between –40 and –60°C, a main negative charge region between –10 and –30°C, a lower positive region near the 0°C layer, and a maximum total charge density approximated to 2 n Cm^{-3}. The simulated results also showed that the squall line presented a dipolar charge structure, and the maximum charge density was less than that in the supercell. During the mature stage of the squall line, the simulated lightning activity was similar to observation.

6. Assimilation of lightning data and forecasting of severe convective weather

Due to a wide detection range, small terrain effects, and continuous observation, lightning data have a potential application in the monitoring, early warning, and forecasting of strong convective weather systems. With the accumulation of high quality lightning location data, lightning data assimilation has become an important research topic.

The exploration of lightning data assimilation methods has received substantial attention. Alexander et al. (1999) were early investigators of lightning data assimilation techniques. They established a relationship between lightning and precipitation ratio with a classic image processing method using microwave sounding data and CG lightning data, and applied it in the MM5 model. This lightning data assimilation technique was shown to improve the 12–24-h precipitation forecast of a superstorm event. Mansell et al. (2007) added NLDN and LMA lightning into the coupled ocean-atmosphere mesoscale prediction system (COAMPS), and utilized lightning data to control the convective parameters of the model, producing simulated precipitation that accurately matched with the observations. Li et al. (2008) obtained a relationship between lightning and convective precipitation by using the TRMM satellite data, and assimilated the convective precipitation retrieved by LIS data into the initial field of the ARPS (Advanced Regional Prediction System) model. To a certain extent, the predicted center and intensity of heavy rain in the Jianghuai region was improved. Based on MM5 model and the lightning and precipitation data of the TRMM satellite, the relation between lightning and precipitation rate was established by Pessi and Businger (2009). They added the relation into the MM5 model, and obtained reasonable results for a low-pressure system in North Pacific. Combining the methods from Papadopoulos et al. (2009) and Mansell et al. (2007), Ran and Zhou (2011) conducted a nudging assimilation of water vapor and cloud hydrometeors using TRMM lightning data. Improvements in short-term rainfall forecasts were achieved for three short-term precipitation events. The distributions of the hydrometeor particles in a thunderstorm play an important role in lightning occurrence. Fierro et al. (2012) established the nudging function of the water vapor mixing ratio and graupel mixing ratio with lightning frequency, and the high-precision lightning data were assimilated into the WRF model. A thunderstorm with a tornado was well simulated, and the convection forecast was significantly improved. Recently, Qie et al. (2014) established empirical relations between total lightning flash rate and the ice particle (graupel, ice, and snow) mixing ratio. The constructed nudging functions were used in the WRF model, and they found that the representation of convection was significantly improved one hour after the total lightning data assimilation, even during the assimilation period. The precipitation center, amount, and coverage were all much closer to the observation in the sensitivity run with lightning data assimilation than in the control run without lightning data assimilation.

Besides the application of lightning data to convective weather forecasting, lightning forecasting itself is also an important issue. Zheng et al. (2005) used lightning data for the Beijing area combined with sounding data, and found that lightning was associated with the potential convective stability index, uplift index, convective available potential energy (CAPE), and potential temperature at 700 hPa. Based on the analysis of the multi-parameter prediction of lightning probability, the diagnostic indicator of lightning forecasting was determined. Strong updraft and sufficient water vapor resulted in more ice particles, which had a direct effect on electrification and discharge (Zheng et al., 2007). Based on the above studies, a lightning monitoring and early warning system was developed by the Chinese Academy of Meteorological Sciences, as described by Zhang et al. (2006b). Based on multiple parameters, multi-algorithms integration technology, and weather forecast products, the potential lightning area and the probability of lightning occurrence in 0–2 h were obtained by the comprehensive prediction method. According to the correlation between lightning density and radar echo, a forecast scheme of CG lightning was established and coupled with the GRAPES model (Wang et al., 2010). It is found that the scheme could forecast the lightning center in 6 h, and the predicted lightning density was consistent with the observation for two thunderstorm cases in South China. McCaul et al. (2009) established a regression equation for prediction of lightning density based on the statistical correlation between ice particles and lightning density. The forecasted lightning zone and trend in 6 h for a supercell storm with a tornado and a hailstorm was consistent with the observations. Barthe et al. (2010) simulated a strong thunderstorm and an air mass thunderstorm in a plateau region using the WRF model. They investigated the lightning forecasting ability by using different physical quantities (falling ice mass, ice water path, and ice quantity flux, updraft, maximum updraft, and cloud top) and obtained decent results. Yair et al. (2010) introduced a new lightning potential index into the WRF model, and forecasted the occurrence of lightning by using the observed lightning data. They found that the forecasting ability for strong convective weather was much improved in predicting the lightning distribution region and the precipitation of three thunderstorms that occurred in the Mediterranean.

7. Conclusion

In this paper, the recent research advances in lightning meteorology are reviewed, with a focus on the research conducted in China. Advanced lightning detection and location technology are summarized, and their important role in the study of lightning meteorology is discussed. Lightning phenomena in different strong convective weather systems such as hailstorm, squall lines, and typhoons are reviewed, and the relationship of lightning and dynamic, microphysical processes and precipitation of thunderstorms are discussed. The charge structure of a thunderstorm is also discussed in terms of both observational and simulation results. The lightning data assimilation method and lightning data application in strong convective weather forecasting are finally elaborated.

The comprehensive understanding of lightning activity is very difficult, because of the complexity in the strong convection weather systems and the differences between individual storms, in addition to the difficulty of accurate detection of lightning. Many scientific questions remain unanswered. The current understanding of lightning activity in different weather systems is still very limited in China. High accuracy and high resolution lightning location technology is crucial for the study of lightning meteorology, and is also the basis of application of lightning data in severe convective weather forecasting. The technology of 3D VHF radiation source location could map lightning discharge with high time and spatial accuracy. The electric field and comprehensive meteorological soundings are the most direct measurement approaches applied to the understanding of electrification in thunderstorms. Both the 3D VHF radiation source location technology and electric field sounding have been well developed in the US, but not in China. Although the LMS, which is similar to the LMA, has been developed by the Cold and Arid Regions Environmental and Engineering Research Institute, Chinese Academy of Sciences (Zhang et al., 2010), there is still no capability of real-time lightning location or monitoring. Research into the electric field sounding of thunderstorms is progressing (Zhao et al., 2009), but only strong electric fields can currently be detected, and the related data are also very limited. Research along this direction should continue to be of high priority in China.

Electrification, lightning, dynamic and microphysical processes in thunderstorms and their relationships are important scientific issues of lightning meteorology. It is very important to study the characteristics of lightning activities in different strong convective weather systems, and also the relationships between the dynamics and the microphysical structure of thunderstorms based on lightning detection and location networks, by using Doppler-polarization radar observations and the electric field sounding inside thunderstorms. The above mentioned issues are the key problems in lightning meteorology today, and will provide the theoretical basis for the application of lightning monitoring in forecasting of strong convective weather.

Lightning data assimilation methods and their application to numerical simulations and predictions will provide supplementary methods to improve short-term severe convective weather forecasting. With the complementary radar data to lightning data, the accuracy of convective activity information in the model initial field could be improved, and the ability of the short-term forecasting of strong convective weather could be further enhanced. This is an important and promising research direction. In addition, carrying out lightning prediction and improving the ability of lightning disaster forecasting will also be an important research direction and application target of lightning meteorology in the future.

REFERENCES

Abarca, S. F., K. L. Corbosiero, D. Vollaro, et al., 2011: The world wide lightning location network and convective activity in tropical cyclones. *Mon. Wea. Rev.*, **139**, 175–191.

Alexander, G. D., J. A. Weinman, V. Karyampudi, et al., 1999: The effect of assimilating rain rates derived from satellites and lightning on forecasts of the 1993 superstorm. *Mon. Wea. Rev.*, **127**, 1433–1457.

Barthe, C., W. Deierling, and M. C. Barth, 2010: Estimation of total lightning from various storm parameters: A cloud-resolving model study. *J. Geophys. Res.*, **115**, D24202, doi: 10.1029/2010JD014405.

Betz, H. D., K. Schmidt, P. Laroche, et al., 2009: LINET—An international lightning detection network in Europe. *Atmos. Res.*, **91**, 564–573.

Biagi, C. J., K. L. Cummins, K. E. Kehoe, et al., 2007: National Lightning Detection Network (NLDN) performance in southern Arizona, Texas, and Oklahoma in 2003–2004. *J. Geophys. Res.*, **112**, D05208, doi: 10.1029/2006JD007341.

Boccippio, D. J., W. J. Koshak, R J. Blakeslee, et al., 2002: Performance assessment of the Optical Transient Detector and Lightning Imaging Sensor. Part I: Predicted diurnal variability. *J. Atmos. Oceanic Technol.*, **19**, 1318–1332.

Bruning, E. C., W. D. Rust, T. J. Schuur, et al., 2007: Electrical and polarimetric radar observations of a multicell storm in TELEX. *Mon. Wea. Rev.*, **135**, 2525–2544.

Carey, L. D., and S. A. Rutledge, 1998: Electrical and multiparameter radar observations of a severe hailstorm. *J. Geophys. Res.*, **103**, 13979–14000.

—, M. J. Murphy, T. L. McCormick, et al., 2005: Lightning location relative to storm structure in a leading-line, trailing-stratiform mesoscale convective system. *J. Geophys. Res.*, **110**, D03105, doi: 10.1029/2003JD004371.

Cao Dongjie, Qie Xiushu, Duan Shu, et al., 2012: Lightning discharge process based on short-baseline lightning VHF radiation source locating system. *Acta Phys. Sinica*, **61**, 510–522. (in Chinese)

Cummins, K. L., M. J. Murphy, E. A. Bardo, et al., 1998: A combined TOA/MDF technology upgrade of the US National Lightning Detection Network. *J. Geophys. Res.*, **103**, 9035–9044.

Dong Wansheng, Liu Xinsheng, Zhang Yijun, et al., 2002: Observations on the leader-return stroke of cloud-to-ground lightning with the broadband interferometer. *Sci. China Earth Sci.*, **45**, 259–269.

Dotzek, N., R. M. Rabin, L. D. Carey, et al., 2005: Lightning activity related to satellite and radar observations of a mesoscale convective system over Texas on 7–8 April 2002. *J. Atmos. Res.*, **76**, 127–176.

Dowden, R. L., R. H. Holzworth, C. J. Rodger, et al., 2008: World-wide lightning location using VLF propagation in the earth-ionosphere waveguide. *IEEE Trans. Antennas Propag.*, **50**, 40–60.

Feng, G. L., X. S. Qie, J. Wang, et al., 2009: Lightning and Doppler radar observations of a squall line system. *Atmos. Res.*, **91**, 466–478.

Feng Guili, Qie Xiushu, and Yuan Tie, 2006: A case study of cloud-to-ground lightning activities in hailstorms under cold eddy synoptic situation. *Acta Meteor. Sinica*, **20**, 489–499.

—, —, —, et al., 2007: Lightning activity and precipitation structure of hailstorms. *Sci. China Earth Sci.*, **50**, 629–639.

Fierro, A. O., E. R. Mansell, C. L. Ziegler, et al., 2012: Application of a lightning data assimilation technique in the WRF-ARW model at cloud-resolving scales for the tornado outbreak of 24 May 2011. *Mon. Wea. Rev.*, **140**, 2609–2627.

Guo Fengxia, Zhang Yijun, and Yan Monghong, 2007: A numerical study of the charge structure in thunderstorm in Nagqu area of the Qinghai-Xizang Plateau. *Chinese J. Atmos. Sci.*, **31**, 28–36. (in Chinese)

Huang Liping, Guan Zhaoyong, Chen Dehui, et al., 2008: Numerical simulation experiments of a thunderstorm process based on a high-resolution mesoscale model. *Chinese J. Atmos. Sci.*, **32**, 1341–1351. (in Chinese)

Lang, T. J., and S. A. Rutledge, 2008: Kinematic, microphysical, and electrical aspects of an asymmetric bow-echo mesoscale convective system observed during STEPS 2000. *J. Geophys. Res.*, **113**, D08213, doi: 10.1029/2006JD007709.

Li, Y. J., G. S. Zhang, J. Wen, et al., 2013: Electrical structure of a Qinghai-Tibetan Plateau thunderstorm based on three-dimensional lightning mapping. *Atmos. Res.*, **127**, 90–115.

Li Wanbiao, Song Guoqiong, and Tong Ke, 2008: Applying TRMM-LIS lightning data to numerical model. *Acta Scientiarum Naturalium Universitatis Pekinensis*, **40**, 399–406. (in Chinese)

Li Wanli, Liu Dongxia, Qie Xiushu, et al., 2012: Evaluation of noninductive charging mechanisms and simulation of charge characteristic structure in the early thunderstorm based on RAMS V6.0. *Acta Phys. Sinica*, **61**, 535–545. (in Chinese)

Liu, D. X., G. L. Feng, and S. J. Wu, 2009: Temporal and spatial characteristics of cloud-to-ground lightning of hailstorms over North China. *Atmos. Res.*, **91**, 459–465.

—, X. S. Qie, L. X. Pan, et al., 2013a: Some characteristics of lightning activity and radiation source distribution in a squall line over North China. *Atmos. Res.*, **132–133**, 423–433.

Liu Dongxia, Qie Xiushu, Xiong Yajun, et al., 2011: Evolution of the total lightning activity in a leading-line and trailing stratiform mesoscale convective system over Beijing. *Adv. Atmos. Sci.*, **28**, 866–878.

—, —, Wang Zhichao, et al., 2013b: Characteristics of lightning radiation source distribution and charge structure of squall line. *Acta Phys. Sinica*, **62**, 219201. (in Chinese)

—, —, Peng Liang, et al., 2014: Charge structure of a summer thunderstorm in North China: Simulation using a regional atmospheric model system. *Adv. Atmos. Sci.*, **31**, 1022–1034, doi: 10.1007/s00376-014-3078-7.

Liu Xinsheng, Ye Zongxiu, Shao Xuanmin, et al., 1989: Intracloud lightning discharge in the lower part of thundercloud. *Acta Meteor. Sinica*, **3**, 212–219.

Lu, G. P., S. A. Cummer, Li J. B., et al., 2009: Charge transfer and in-cloud structure of large-charge-moment positive lightning strokes in a mesoscale convective system. *Geophys. Res. Lett.*, **36**, L15805, doi: 10.1029/2009GL038880.

Lü Fanchao, Zhu Boyou, Ma Ming, et al., 2013: Observations of narrow bipolar events during two thunderstorms in Northeast China. *Sci. China Earth Sci.*, **56**, 1459–1470.

Ma Ming, Lin Jinbing, and Fu Yunfei, 2012: A study of lightning and precipitation profiles of a severe convective activity. *Acta Meteor. Sinica*, **70**, 797–805. (in Chinese)

MacGorman, D. R., W. D. Rust, P. Krehbiel, et al., 2005: The electrical structure of two supercell storms during STEPS. *Mon. Wea. Rev.*, **133**, 2583–2607.

Mansell, E. R., D. R. MacGorman, C. L. Ziegler, et al., 2002: Simulated three-dimensional branched lightning in a numerical thunderstorm model. *J. Geophys. Res.*, **107**, ACL 2-1-ACL 2-12, doi: 10.1029/2000JD000244.

—–, —–, C. L. Ziegler, et al., 2005: Charge structure and lightning sensitivity in a simulated multicell thunderstorm. *J. Geophys. Res.*, **110**, D12101, doi: 10.1029/2004JD005287.

—–, C. L. Ziegler, and D. R. MacGorman, 2007: A lightning data assimilation technique for mesoscale forecast models. *Mon. Wea. Rev.*, **135**, 1732–1748.

Marshall, T. C., W. D. Rust, and M. Stolzenburg, 1995: Electrical structure and updraft speeds in thunderstorms over the southern great plains. *J. Geophys. Res.*, **100**, 1001–1015.

McCaul, E. W., S. J. Goodman, K. M. LaCasse, et al., 2009: Forecasting lightning threat using cloud-resolving model simulations. *Wea. Forecasting*, **24**, 709–729.

Molinari, J., P. K. Moore, V. P. Idone, et al., 1994: Cloud-to-ground lightning in Hurricane Andrew. *J. Geophys. Res.*, **99**, 16665–16676.

Pan Lunxiang, Qie Xiushu, Liu Dongxia, et al., 2010: The lightning activities in super typhoons over the Northwest Pacific. *Sci. China Earth Sci.*, **53**, 1241–1248.

—–, —–, Zhu Runpeng, et al., 2013: Land-sea contrast in the lightning diurnal variation as observed by the WWLLN and LIS/OTD data. *Acta Meteor. Sinica*, **27**, 591–600.

—–, —–, and Wang Dongfang, 2014: Lightning activity and its relation to the intensity of typhoons over the Northwest Pacific Ocean. *Adv. Atmos. Sci.*, **31**, 581–592, doi: 10.1007/s00376-013-3115-y.

Papadopoulos, A., E. Serpetzoglou, and E. N. Anagnostou, 2009: Evaluating the impact of lightning data assimilation on mesoscale model simulations of a flash flood inducing storm. *Atmos. Res.*, **94**, 715–725.

Pasko, V. P., M. A. Stanley, and J. D. Mathews, 2002: Electrical discharge from a thundercloud top to the lower ionosphere. *Nature*, **416**, 152–154.

Parker, M. D., S. A. Rutledge, and R. H. Jonson, 2000: Cloud-to-ground lightning in linear mesoscale convective systems. *Mon. Wea. Rev.*, **129**, 1232–1241.

Pessi, A. T., and S. Businger, 2009: The impact of lightning data assimilation on a winter storm simulation over the North Pacific Ocean. *Mon. Wea. Rev.*, **137**, 3177–3195.

Price, C., M. Asfur, and Y. Yair, 2009: Maximum hurricane intensity preceded by increase in lightning frequency. *Nature Geoscience*, **2**, 329–332.

Qie, X. S. T. L. Zhang, C. P. Chen, et al., 2005: The lower positive charge center and its effect on lightning discharges on the Tibetan Plateau. *Geophys. Res. Lett.*, **32**, doi: 10.1029/2004GL022162.

—–, T. L. Zhang, G. S. Zhang, et al., 2009: Electrical characteristics of thunderstorms in different plateau regions of China. *Atmos. Res.*, **91**, 244–249.

—–, R. P. Zhu, T. Yuan, et al., 2014: Application of total-lightning data assimilation in a mesoscale convective system based on the WRF model. *Atmos. Res.*, 145–146, 255–266.

Qie Xiushu, 2012: Progresses in the atmospheric electricity researches in China during 2006–2010. *Adv. Atmos. Sci.*, **29**, 993–1005.

—–, Monghong Yan, Guo Changming, et al., 1993: Lightning data and study of thunderstorm nowcasting. *Acta Meteor. Sinica*, **7**, 244–256.

—–, Zhang Yijun, and Zhang Qilin, 2006: Study on the characteristics of lightning discharges and the electric structure of thunderstorms. *Acta Meteor. Sinica*, **20**, 244–257.

—–, Zhang Qinlin, Yuan Tie, et al., 2013: *Lightning and Physics*. Science Press, Beijing, 297 pp. (in Chinese)

Ran Lingkun and Zhou Yushu, 2011: Application of lightning observations of TRMM satellite to the mesoscale numerical model by a new nudging assimilation adjustment technique. *Chinese J. Atmos. Sci.*, **35**, 1145–1158. (in Chinese)

Reap, R. M., and D. R. MacGorman, 1989: Cloud-to-ground lightning: Climatological characteristics and relationships to model fields, radar observations, and severe local 796 storms. *Mon. Wea. Rev.*, **117**, 518–535.

Richard, P., A. Delannoy, and G. Labaune, 1986: Results of spatial and temporal characterization of VHF-UHF radiation of lightning. *J. Geophys. Res.*, **91**, 1248–1260.

Rison, W. R., R. J. Thomas, P. R. Krehbiel, et al., 1999: A GPS-based three-dimensional lightning mapping system: Initial observations in central New Mexico. *Geophys. Res. Lett.*, **26**, 3573–3576.

Saunders, C. P. R., W. D. Keith, and R. P. Mitzeva, 1991: The effect of liquid water on thunderstorm charging. *J. Geophys. Res.*, **96**, 11007–11017.

——, and S. L. Peck, 1998: Laboratory studies of the influence of the rime accretion rate on charge transfer during crystal/graupel collisions. *J. Geophys. Res.*, **103**, 13949–13956.

Schultz, C. J., W. A. Peterson, and L. D. Carey, 2011: Lightning and severe weather: A comparison between total and cloud-to-ground lightning trends. *Wea. Forecasting*, **26**, 744–755.

Simpson, G., and F. J. Scrase, 1937: The distribution of electricity in thunderclouds. *Proc. Roy. Soc. London, Ser. A*, **161**, 309–352.

Smith, D. A., X. M. Shao, D. N. Holden, et al., 1999: A distinct class of isolated intracloud lightning discharges and their associated radio emissions. *J. Geophys. Res.*, **104**, 4189–4212.

——, K. B. Eack, J. Harlin, et al., 2002: The Los Alamos Sferic Array: A research tool for lightning investigations. *J. Geophys. Res.*, **107**, 4183, doi: 10.1029/2001JD000502.

Soula, S., Y. Seity, L. Feral, et al., 2004: Cloud-to-ground lightning activity in hail-bearing storms. *J. Geophys. Res.*, **109**, 2101–2113.

Stolzenburg, M., W. D. Rust, and T. C. Marshall, 1998: Electrical structure in thunderstorm convective regions: 3. Synthesis. *J. Geophys. Res.*, **103**, 14097–14108.

Sun Anping, Yan Muhong, Zhang Yijun, et al., 2002: Numerical study of thunderstorm electrification with a three dimensional dynamics and electrification coupled model I: Model description and parameterization of electrical processes. *Acta Meteor. Sinica*, **60**, 722–731. (in Chinese)

Sun, Z. L., X. S. Qie, M. Y. Liu, et al., 2013: Lightning VHF radiation location system based on short-baseline TDOA technique—Validation in rocket-triggered lightning. *Atmos. Res.*, 129–130, 58–66.

Takahashi, T., 1978: Riming electrification as a charge generation mechanism in thunderstorms. *J. Atmos. Sci.*, **35**, 1536–1548.

Tan, Y. B., S. C. Tao, and B. Y. Zhu, 2006: Fine-resolution simulation of the channel structures and propagation features of intracloud lightning. *Geophys. Res. Lett.*, **33**, L09809, doi: 10.1029/2005GL025523.

Tan Yongbo, Tao Shanchang, Zhu Baoyou, et al., 2007: A simulation of the effects of intra-cloud lightning discharges on the charges and electrostatic potential distributions in a thundercloud. *Chinese J. Geophys.*, **50**, 1053–1065. (in Chinese)

Tessendorf, S. A., S. A. Rutledge, and K. C. Wiens, 2007: Radar and lightning observations of normal and inverted polarity multicellular storms from STEPS. *Mon. Wea. Rev.*, **135**, 3682–3706.

Wang Dongfang, Qie Xiushu, Yuan Tie, et al., 2009: An analysis of the initial stage of intracloud lightning using the pulse location technique based on the fast electric field change. *Acta Meteor. Sinica*, **23**, 772–781.

Wang Fei, Zhang Yijun, and Dong Wansheng, 2010: A lightning activity forecast scheme developed for summer thunderstorms in South China. *Acta Meteor. Sinica.*, **24**, 631–640.

Wang, Y. H., G. S. Zhang, X. S. Qie, et al., 2012: Characteristics of compact intracloud discharges observed in a severe thunderstorm in northern part of China. *J. Atmos. Sol-Terr. Phys.*, 84–85, 7–14.

Wu, T., W. S. Dong Y. J. Zhang, et al., 2011: Comparison of positive and negative compact intracloud discharges. *J. Geophys. Res.*, **116**, D03111, doi: 10.1029/2010JD015233.

——, ——, L. F. Li, et al., 2012: 3D location of compact intracloud discharge based on its ionospheric reflection pair. *Chinese J. Geophys.*, **55**, 1095–1103. (in Chinese)

Xu Liangtao, Zhang Yijun, Wang Fei, et al., 2012: Coupling of electrification and discharge processes with WRF model and its preliminary verification. *Chinese J. Atmos. Sci.*, **36**, 1041–1052. (in Chinese)

Yair, Y., B. Lynn, C. Price, et al., 2010: Predicting the potential for lightning activity in mediterranean storms based on the Weather Research and Forecasting (WRF) model dynamic and microphysical fields. *J. Geophys. Res.*, **115**, D04205, doi: 10.1029/2008JD010868.

Yan Muhong, Guo Changming, Ge Zhengmo, et al., 1996: Numerical study of cloud dynamic-electrification in axisymmetric, time-depended cloud model. Part I:

Theory and model. *Acta Geophy. Sinica*, **39**, 52–64. (in Chinese)

Yang Meirong, Yuan Tie, Qie Xiushu, et al., 2011: An analysis of the characteristics of lightning activities, radar reflectivity and ice scattering for tropical cyclones over the western North Pacific. *Acta Meteor. Sinica*, **69**, 646–658. (in Chinese)

Yang Jing, Qie Xiushu, Zhang Guangshu, et al., 2008: Red sprites over thunderstorms in the coast of Shandong Province, China. *Chin. Sci. Bull.*, **53**, 1079–1086, doi: 10.1007/s11434-008-0141-8.

——, Yang Meirong, Liu Chao, et al., 2013a: Case studies of sprite-producing and non-sprite-producing summer thunderstorms. *Adv. Atmos. Sci.*, **30**, 1786–1808.

Yang, J., X. S. Qie, and G. L. Feng, 2013b: Characteristics of one sprite-producing summer thunderstorm. *Atmos. Res.*, **127**, 90–115.

Yao Wen, Zhang Yijun, Meng Qing, et al., 2013: A comparison of the characteristics of total and cloud-to-ground lightning activities in hailstorms. *Acta Meteor. Sinica*, **27**, 282–293.

Yuan, T., and X. S. Qie, 2008: Study on lightning activity and precipitation characteristics before and after the onset of the South China Sea summer monsoon. *J. Geophys. Res.*, **113**, D14101, doi: 10.1029/2007JD009382.

Yuan Tie and Qie Xiushu, 2010a: TRMM-based study of lightning activity and its relationship with precipitation structure of a squall line in South China. *Chinese J. Atmos. Sci.*, **34**, 58–70. (in Chinese)

—— and ——, 2010b: Characteristics of the lightning activity, radar reflectivity, and microwave brightness temperature of warm season precipitation systems over the eastern China and adjacent seas as observed by TRMM satellite. *Acta Meteor. Sinica*, **68**, 652–665. (in Chinese)

Zhang Guangshu, Zhao Yuxiang, Qie Xiushu, et al., 2008: Observation and study on the whole process of cloud-to-ground lightning using narrowband radio interferometer. *Sci. China Earth Sci.*, **51**, 694–708.

——, Wang Yanhui, Qie Xiushu, et al., 2010: Using lightning locating system based on time-of-arrival technique to study three-dimensional lightning discharge processes. *Sci. China Earth Sci.*, **53**, 591–602.

Zhang Wenjuan, Zhang Yijun, Zheng Dong, et al., 2012: Lightning distribution and eyewall outbreaks in tropical cyclones during landfall. *Mon. Wea. Rev.*, **140**, 3573–3586.

Zhang Yijun, Yan Muhong, Zhang Cuihua, et al., 2000: Simulating calculation of charge structure in thunderstorm for different areas. *Acta Geophy. Sinica*, **58**, 617–627. (in Chinese)

——, Meng Qing, P. R. Krehbiel, et al., 2004: Spatial and temporal characteristics of VHF radiation source produced by lightning in supercell thunderstorms. *Chin. Sci. Bull.*, **49**, 624–631.

——, ——, Lu Weitao, et al., 2006a: Charge structures and cloud-to-ground lightning discharges characteristics in two supercell thunderstorms. *Chin. Sci. Bull.*, **51**, 198–212.

——, ——, Ma Ming, et al., 2006b: Development of lightning detection technique with application of lightning data. *J. Appl. Meteor. Sci.*, **17**, 611–620. (in Chinese)

Zhao Zhongkuo, Qie Xiushu, Zhang Tinglong, et al., 2009: Electric field soundings and the charge structure within an isolated thunderstorm. *Chin. Sci. Bull.*, **55**, 872–876.

Zheng, D., Y. J. Zhang, Q. Meng, et al., 2010: Lightning activity and electrical structure in a thunderstorm that continued for more than 24 h. *Atmos. Res.*, **97**, 241–256.

Zheng Dong, Zhang Yijun, Lü Weitao, et al., 2005: Atmospheric instablity parameters and forecasting of lightning activity. *Plateau Meteor.*, **24**, 196–203. (in Chinese)

——, ——, Ma Ming, et al., 2007: Simulation study on the influence of atmospheric stratification on lightning activity. *Acta Meteor. Sinica*, **65**, 622–632. (in Chinese)

Zheng Yuanyuan, Fu Yunfei, Liu Yong, et al., 2004: Heavy rainfall structures and lightning activities in a cold-front cyclone happened in Huai River derived from TRMM PR and LIS observations. *Acta Meteor. Sinica*, **62**, 790–802. (in Chinese)

Zhou, Y. J., X. S. Qie, and S. Soula, 2002: A study of the relationship between cloud-to-ground lightning and precipitation in the convective weather system in China. *Annales Geophysicae*, **20**, 107–113.

Zhou Yunjun, Qie Xiushu, Zhang Yijun, et al., 1999: The relationship between cloud to ground lightning and precipitation in the convective weather. *Acta Meteor. Sinica*, **57**, 103–111. (in Chinese)

Zhou Zhiming and Guo Xueliang, 2009: A three-dimensional modeling study of multi-layer distribution and formation processes of electric charges in a severe thunderstorm. *Chinese J. Atmos. Sci.*, **33**, 600–620. (in Chinese)

Zhu, B. Y. H. L. Zhou, M. Ma, et al., 2010: Observations of narrow bipolar events in East China. *J. Atmos. Sol-Terr. Phys.*, **72**, 271–278.

Zhu Baoyou, Tao Shanchang, and Tan Yongbo, 2007: Initial observations of the lightning narrow bipolar pulses with very powerful VHF radiation. *Acta Meteor. Sinica*, **65**, 124–130. (in Chinese)

Zhu Runpeng, Yuan Tie, and Li Wanli, 2013: Characteristics of global lightning activities based on satellite observations. *Climatic Environ. Res.*, **18**, 639–650. (in Chinese)